

Structural Evolution and Amorphization Kinetics of Copper Nanorods Under Thermal Annealing: A Molecular Dynamics Insight

Nguyen Dac Dien ^{1,*}, Bui Thi Phuong Hoa ², Lam Vu Truong ³, Umut Saraç ⁴,

¹ Faculty of Occupational Safety and Health, Vietnam Trade Union University, 169 Tay Son, Kim Lien, 100000, Hanoi, Vietnam.

² Faculty of Applied Sciences, University of Transport Technology, 54 Trieu Khuc, Thanh Xuan, Hanoi, 100000, Vietnam.

³ Department of Advanced Materials and Metallurgical Engineering, Sunchon National University, Suncheon, Jeonnam 540-742, Republic of Korea.

⁴ Bartın University, Department of Science Education, 74100, Bartın, Türkiye.

Article info

Type of articles:

Original article

Corresponding author*:

Nguyen Dac Dien:
diennd@dhcd.edu.vn

Received: 14 May 2026

Revised: 11 June 2026

Accepted: 14 June 2026

Published: 28 June 2026

Abstract: This study employs molecular dynamics (MD) simulations to investigate the effects of temperature (600, 650, and 700 K) and annealing time (0-32 ps) on the atomic structure of copper nanorods. The embedded atom method (EAM) potential is used to model interatomic interactions under NPT conditions. Structural evolution is characterized using radial distribution function (RDF), coordination number, common neighbor analysis (CNA), and total energy. Results reveal that increasing temperature induces structural disorder, with a gradual transformation from a highly ordered Face-Centered Cubic (FCC) lattice to a partially amorphous state. Conversely, prolonged annealing promotes atomic rearrangement and recrystallization, stabilizing the structure. At 650 K and ~28 ps, the system achieves optimal stability with the lowest energy and highest FCC fraction. These findings provide atomistic insights into thermal treatment optimization of copper-based materials and contribute to the understanding of thermally induced structural evolution in metallic systems.

Keywords: Copper nanorods, Molecular dynamics simulation, Structural evolution, Amorphization kinetics

1. Introduction

Copper (Cu) is one of the most widely used metallic materials in engineering and technological applications due to its excellent electrical conductivity, thermal conductivity, and corrosion resistance [1-

7]. Its performance in practical applications, however, is strongly dependent on its microstructure, which can be significantly altered through thermal treatments such as annealing. Annealing is a crucial process that enables recovery, recrystallization, and grain growth, thereby influencing both mechanical and physical properties of copper-based materials [8-13]. At elevated temperatures, atomic diffusion becomes more active, leading to structural rearrangement and defect annihilation. Temperature drives the atomic mobility and provides the thermal energy required for atoms to overcome local energy barriers, leading to either defect annihilation or structural collapse. Concurrently, the annealing time governs the kinetic window allowed for these atomic rearrangements. Understanding the coupling effect of these two parameters is crucial for controlling the crystalline-to-amorphous transitions in low-dimensional copper nanostructures. These processes are governed not only by temperature but also by the duration of annealing, which determines the extent of atomic mobility and structural stabilization [14–17]. In particular, the competition between thermal disordering and recrystallization plays a key role in defining the final atomic configuration. While higher temperatures tend to destabilize the crystalline lattice and promote amorphization, sufficient annealing time can facilitate the reorganization of atoms into more stable configurations [1, 2, 18]. In recent years, molecular dynamics (MD) simulation has emerged as a powerful tool for investigating the atomic-scale mechanisms underlying thermal processes in metallic systems. Unlike experimental techniques, MD simulations allow for direct observation of atomic motion and structural evolution with high temporal and spatial resolution [3-5, 19]. This approach has been successfully applied to study phase transitions, defect dynamics, and recrystallization behavior in various metals, including copper [6, 20, 21]. Key structural descriptors such as radial distribution function (RDF), coordination number, and common neighbor analysis (CNA) provide quantitative insights into changes in atomic ordering and phase composition during thermal treatment [22-25]. Several studies have investigated the influence of temperature on the structural stability of copper, demonstrating that increasing temperature leads to enhanced atomic vibrations, reduced long-range order, and eventual structural degradation [26-28]. Meanwhile, the effect of annealing time has been associated with kinetic processes such as grain boundary migration and defect healing, which contribute to the stabilization of the crystal structure [29-32]. However, most existing works focus on either temperature or annealing time independently, and a comprehensive understanding of their combined effects, particularly within the intermediate temperature range of 600-700 K and short annealing times at the picosecond scale, remains limited [29-31, 33]. Furthermore, recent MD studies, including those by Nguyen Trong Dung and co-workers, have highlighted the importance of analyzing the interplay between Face-Centered Cubic (FCC) stability, Hexagonal Close-Packed (HCP) formation, and amorphous phase evolution under thermal conditions [34-37]. These structural transformations are critical for understanding the fundamental mechanisms governing the thermodynamic stability and mechanical performance of copper at the nanoscale. Therefore, the present study aims to systematically investigate the combined effects of temperature (600, 650, and 700 K) and annealing time (0-32 ps) on the atomic structure of copper nanorods using molecular dynamics simulations. By analyzing structural evolution through RDF, CNA, coordination number, and energy variations, this work seeks to identify optimal thermal conditions that balance structural stability and atomic mobility. While numerous molecular dynamics studies have addressed the thermal stability of bulk copper or copper nanoparticles, the structural evolution of Cu nanorods remains less understood. The high aspect ratio and unique surface-to-volume ratio of nanorods induce distinct surface stress profiles that alter the kinetics of phase

transitions. This work addresses this scientific gap by uncovering the atomic-scale mechanisms governing defect elimination and structural preservation under spatial confinement. Despite extensive investigations on thermal stability in Cu nanoparticles and nanorods, the kinetic pathway governing amorphization and recrystallization in Cu nanorods remains unclear. In particular, the competition between surface-energy-driven disordering and thermally activated defect annihilation has not been quantitatively established. Therefore, this study investigates the temperature–time dependent structural evolution for Cu nanorods and identifies the critical thermal conditions governing the transition from crystalline FCC structures to partially amorphous states. The findings are expected to provide valuable insights for optimizing thermal treatment processes and improving the performance of copper-based materials in advanced applications.

2. Methodology

2.1. Model Construction

A copper (Cu) nanorod model was constructed based on a Face-Centered Cubic (FCC) lattice with a lattice constant of 3.615 Å. The initial simulation cell had approximate dimensions of 10 × 10 × 20 nm, containing about 100,000 atoms to ensure statistical reliability while maintaining computational efficiency. Periodic boundary conditions were applied only along the z-direction, whereas free surfaces were preserved in the x and y directions by introducing vacuum layers. The initial configuration was generated using a perfect FCC crystal structure, followed by geometric relaxation to remove any artificial stresses introduced during model construction.

2.2. Interatomic Potential

Atomic interactions were described using the Embedded Atom Method (EAM) potential, which is widely recognized for accurately capturing the many-body interactions in metallic systems. The EAM potential accounts for both pairwise interactions and electron density contributions, making it suitable for simulating structural evolution, defect formation, and phase transitions in copper [22-24]. The embedded-atom method (EAM) potential developed by Mishin et al [38] was employed, which has been well-validated for reproducing the lattice constants, elastic properties, and stacking fault energies of Cu. To eliminate high-frequency thermal noise and ensure statistical reliability, the structural metrics (RDF, CNA, and CN) were calculated using a time-averaging procedure sampled every 0.1 ps over the final 5ps of each annealing window.

2.3. Simulation Parameters

All molecular dynamics simulations were performed using a time step of 1 fs to ensure numerical stability. The system was simulated under the isothermal–isobaric (NPT) ensemble, where both temperature and pressure were controlled. Temperature control: Nose–Hoover thermostat Pressure control: Nose–Hoover barostat ($P = 0$ GPa). Integration algorithm: Velocity-Verlet. Cutoff radius: ~ 10 Å. Simulation software: LAMMPS (widely used MD package). Before thermal treatment, the system was equilibrated at 300 K for 100 ps to reach a stable initial state.

2.4. Simulation Procedure

The simulation process consisted of four main stages:

Energy Minimization: The initial structure was relaxed using the conjugate gradient method until the energy convergence criterion of 10^{-6} eV was achieved. This step ensured removal of residual stresses and attainment of a stable starting configuration.

Heating Process: The system was gradually heated from 300 K to target temperatures (600 K, 650 K, and 700 K) with a heating rate of approximately 10 K/ps to avoid thermal shock and non-physical structural distortion.

Annealing Process: At each target temperature, the system was annealed for different durations: 0, 7, 14, 21, 28, and 32 ps. During annealing, temperature and pressure were maintained constant under the NPT ensemble to allow atomic diffusion and structural evolution.

Cooling and Stabilization: After annealing, the system was cooled down to 300 K to freeze the atomic configuration and enable structural analysis. A short equilibration (~50 ps) was performed to ensure stability of the final structure.

The temperature range of 600-700 K was selected because it represents the thermally activated regime below the melting temperature of this specific nanorod (850K). The annealing time of 0-32 ps is sufficient to capture the ultra-fast structural relaxation driven by surface energy minimization in nanomaterials, after which the system reaches a quasi-steady state.

2.5. Structural Characterization Methods

To analyze the structural evolution of the copper nanorod, several quantitative metrics were employed:

Radial Distribution Function (RDF), $g(r)$: Used to evaluate short-range and long-range atomic ordering. Changes in peak intensity and position indicate structural transitions.

Common Neighbor Analysis (CNA): Applied to identify local atomic environments, including FCC, HCP, and amorphous structures. In addition, the centrosymmetry parameter (CSP) was employed to quantify local lattice distortions and defect accumulation. CSP enables sensitive detection of deviations from the ideal FCC environment and provides complementary information to CNA regarding thermally induced disorder. This method provides insight into phase transformation and defect formation.

Coordination Number (CN): Calculated to assess the average number of nearest neighbors, reflecting structural compactness and disorder.

Total Energy per Atom: Used to evaluate system stability and monitor thermodynamic evolution during annealing.

Atomic Configuration Visualization: Visualization tools such as OVITO were used to observe atomic arrangements and identify defects, grain boundaries, and phase transitions.

2.6. Data Analysis and Reproducibility

All simulations were repeated at least three times with different initial velocity distributions to ensure reproducibility. The reported results represent averaged values to minimize statistical fluctuations. The methodology adopted in this study follows well-established MD simulation frameworks and is consistent with recent works on thermal effects in metallic systems, including studies on copper and related materials [26-31 34-38].

3. Results and Discussion

3.1. Atomic Structural Characteristics

The structural evolution of the copper nanorod under different thermal conditions was first examined using the radial distribution function (RDF), coordination number (CN), and common neighbor analysis (CNA). These metrics provide complementary insights into both short-range and long-range atomic ordering [39]. At the initial state (300 K), the RDF exhibits sharp and well-defined peaks corresponding to the characteristic interatomic distances of a face-centered cubic (FCC) lattice. The first peak, located at approximately 2.55 Å, represents the nearest-neighbor distance in copper, while subsequent peaks

indicate long-range periodicity. The high intensity and narrow width of these peaks confirm the highly ordered crystalline structure. As the system is heated to elevated temperatures, significant changes in the RDF profiles are observed [26-28, 40]. Specifically, the peak intensities decrease and broaden, indicating increased atomic vibrations and a gradual loss of long-range order. This effect becomes more pronounced at higher temperatures, particularly at 700 K, where the second and third RDF peaks begin to merge, suggesting partial amorphization. The coordination number analysis further supports this observation. At low temperature, the average CN remains close to 12, which is characteristic of the FCC structure. However, with increasing temperature, the CN distribution becomes broader, indicating the presence of local structural distortions and defects. CNA results reveal a clear transition in atomic configurations. At 600 K, FCC atoms dominate the structure, accounting for more than 90% of the total atoms. At 650 K, a slight increase in HCP atoms is observed, indicating the formation of stacking faults and twin boundaries. At 700 K, the fraction of FCC atoms decreases significantly, while amorphous atoms increase, reflecting the onset of structural disorder. These findings demonstrate that temperature plays a critical role in destabilizing the crystalline lattice by enhancing atomic mobility and disrupting periodic ordering. The observed trends are consistent with previous MD studies on metallic systems, where thermal fluctuations lead to structural transitions from ordered to disordered states.

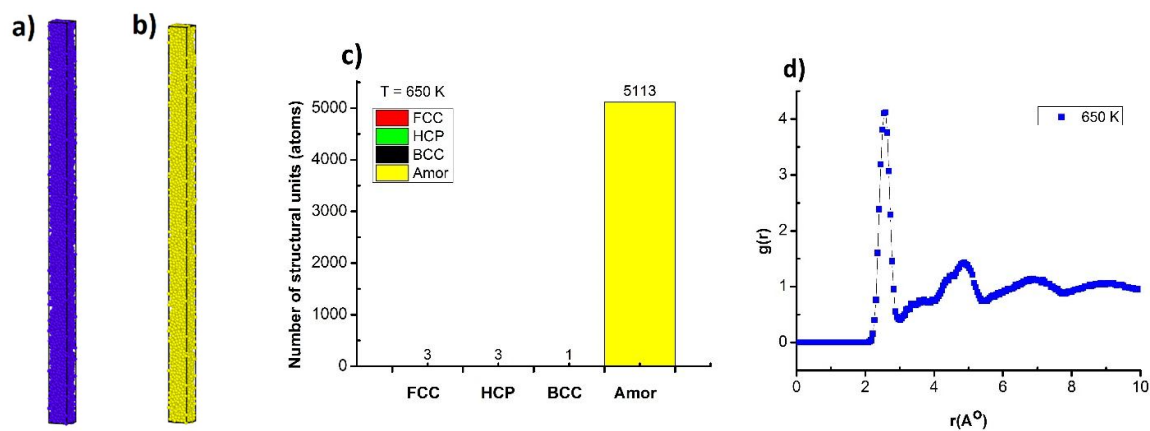


Figure 1. Initial atomic configuration (a), CNA-colored atomic structure (b), CNA statistics (c), and RDF profile (d) of the Cu nanorod annealed at 650 K for 28 ps.

3.2. Effect of Temperature

Temperature is a primary factor influencing atomic motion, energy distribution, and structural stability in metallic systems. In this study, the effect of temperature was systematically investigated at 600 K, 650 K, and 700 K. At 600 K, the copper nanorod retains a largely stable FCC structure. Although thermal vibrations are present, they are not sufficient to significantly disrupt the lattice. The RDF peaks remain well-defined, and the CNA analysis confirms that the majority of atoms are in FCC configurations. Minor deviations from perfect crystallinity are attributed to thermal fluctuations rather than structural transformation. At 650 K, the nanorod exhibits pronounced structural reorganization. The increased thermal energy enhances atomic mobility, allowing atoms to overcome local energy barriers and rearrange into more energetically favorable configurations. This results in a reduction of defects such as vacancies and dislocations, leading to a more uniform structure. Interestingly, while some local disorder is introduced, the overall structural stability improves due to defect annihilation and atomic

reorganization. The total energy analysis shows that the system reaches a relatively low energy state at this temperature, indicating a balance between thermal activation and structural stability.

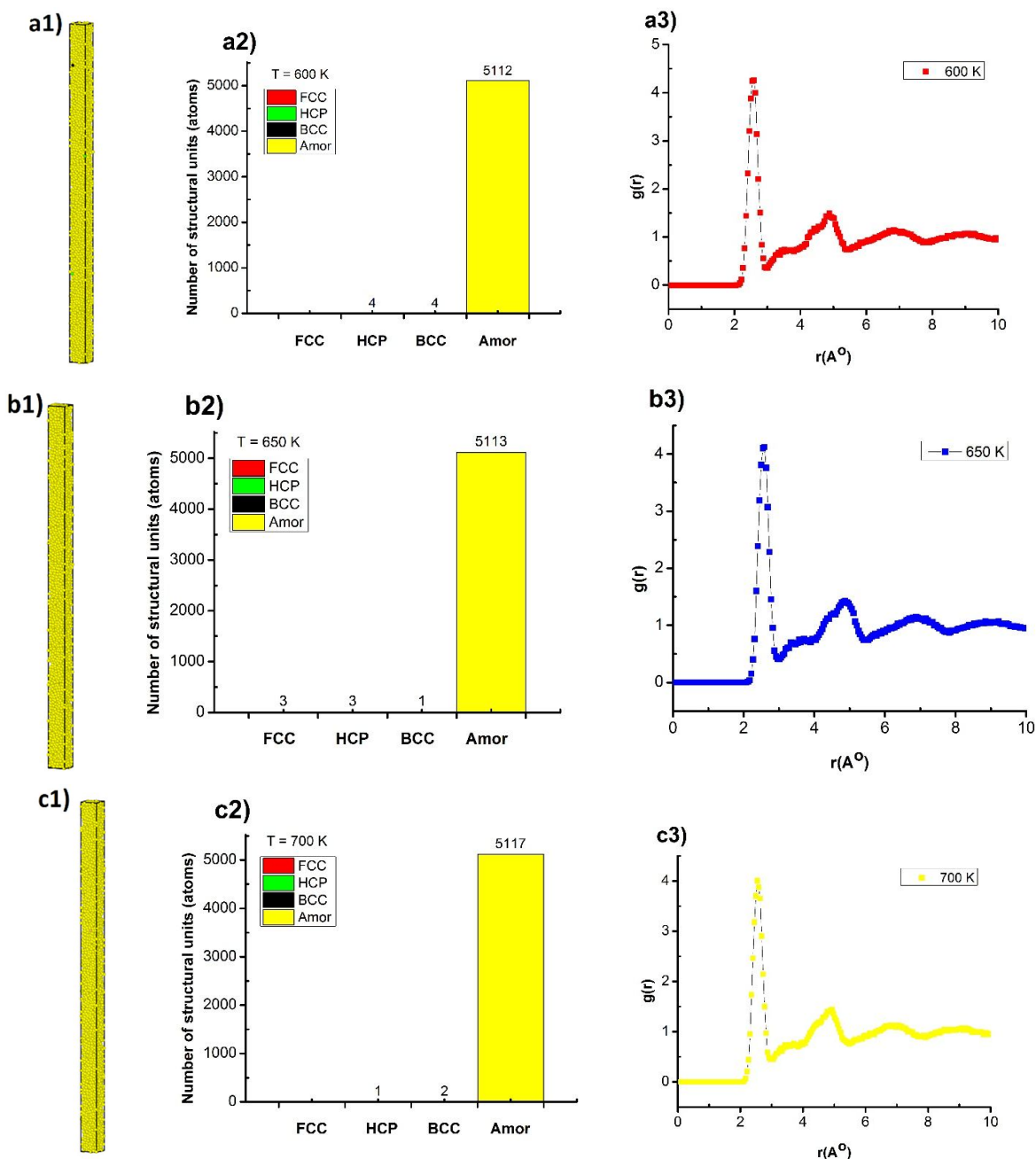


Figure 2 Atomic configurations (a1–c1), CNA statistics (a2–c2), and RDF profiles (a3–c3) of Cu nanorods at different annealing temperatures after 28 ps.

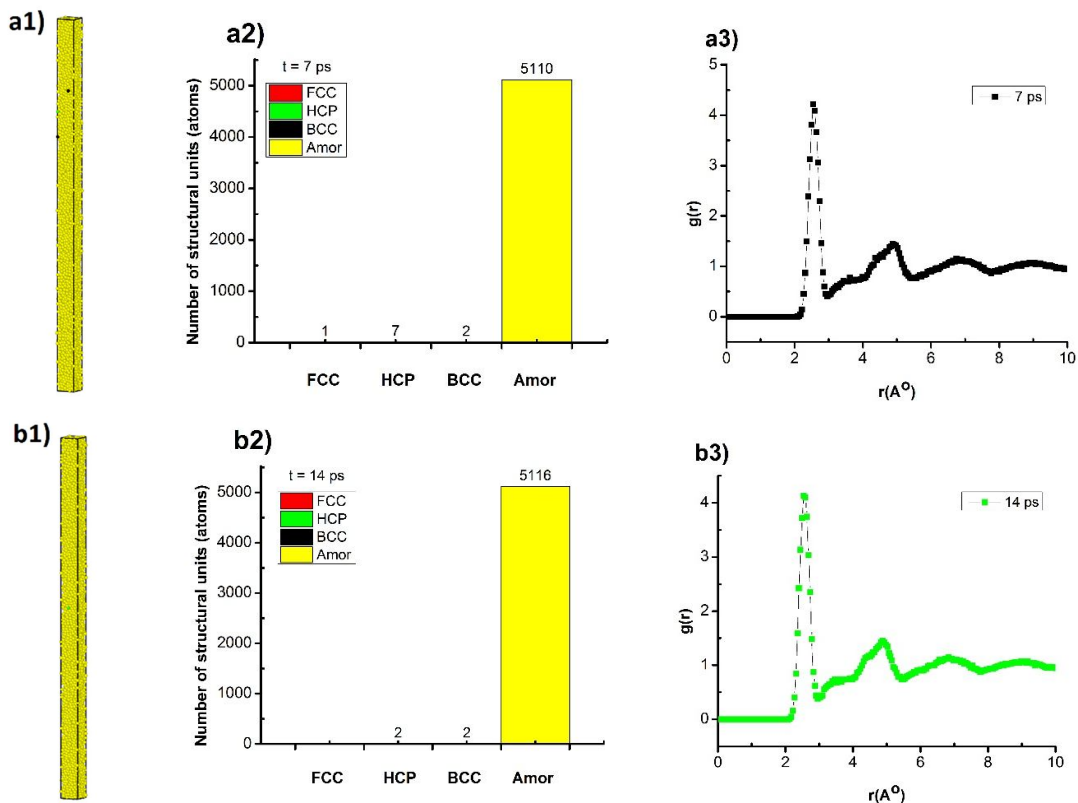
This suggests that 650 K represents an optimal temperature for annealing, where the system can effectively reorganize without undergoing excessive disorder. At 700 K, the system exhibits significant structural degradation. The RDF peaks become broader and less distinct, indicating a loss of long-range order. CNA results show a substantial decrease in FCC atoms and a corresponding increase in amorphous structures. The high thermal energy at this temperature leads to excessive atomic vibrations, which disrupt the lattice and promote disorder. Furthermore, the total energy per atom increases significantly at 700 K, reflecting the unstable nature of the system. The increased energy indicates that the system is

far from equilibrium and is undergoing continuous structural fluctuations. Overall, the results demonstrate a non-linear relationship between temperature and structural stability. While moderate temperature (650 K) enhances structural optimization, excessive temperature (700 K) leads to degradation and loss of crystallinity. The existence of the amorphous state under periodic boundary conditions is attributed to the nanoscale size effect and high surface stress. Although PBC is applied, the presence of large vacuum padding along the x and y axes creates an isolated nanorod geometry with an extremely high surface-to-volume ratio. The surface atoms possess low coordination numbers and high excess free energy. At elevated temperatures (600–700 K), this intense surface stress acts as a driving force that disrupts the interior FCC lattice, triggering a structural transition into a metastable amorphous state to minimize the total surface energy of the nanorod.

Diffusion Behavior: The atomic mobility was further quantified through the mean square displacement (MSD). The MSD curves increase progressively with temperature, indicating enhanced atomic diffusion. At 700 K, the MSD exhibits a sharp rise, suggesting the onset of collective atomic rearrangements associated with partial amorphization. In contrast, the moderate increase observed at 650 K reflects sufficient atomic mobility for defect healing without extensive structural collapse.

3.3. Effect of Annealing Time

In addition to temperature, annealing time plays a crucial role in determining the extent of atomic diffusion and structural evolution [29-31]. The effect of annealing time was investigated at intervals of 0, 7, 14, 21, 28, and 32 ps. The results show that at $t = 7$ ps, the Cu nanorod has the structural shape (Figure 3a1), with the corresponding number of structural units 1 FCC, 7 HCP, 2 BCC, 1510 Amor (Figure 3a2) and a radial distribution function with a Cu-Cu bond length of 2.54 Å, and a radial distribution function height $g(r) = 4.22$ (Figure 3a3).



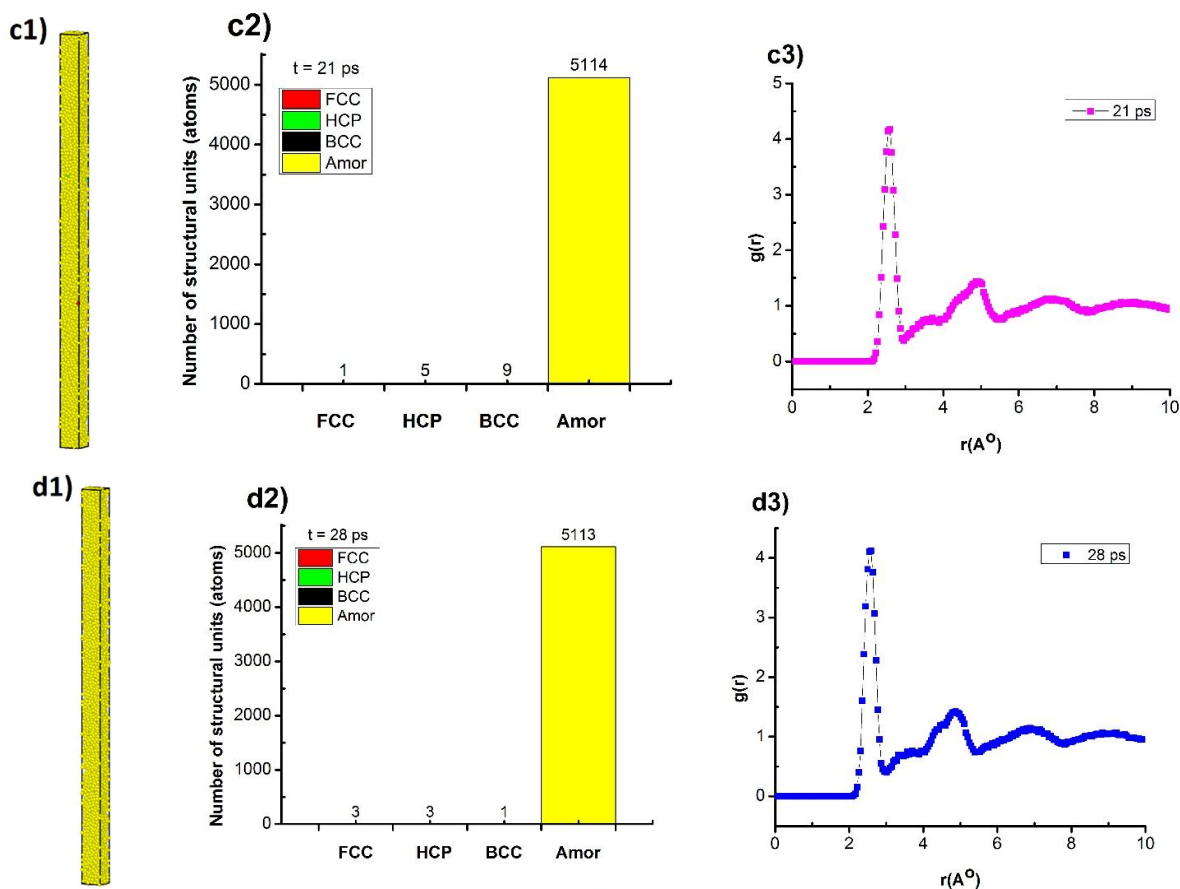


Figure 3 Structural shape (a1, b1, c1, d1), number of structural units (a2, b2, c2, d2), and radial distribution function (a3, b3, c3, d3) of Cu nanorods at 650 K with different annealing times.

When increasing the annealing time from $t = 7$ ps to $t = 14, 21, 28$ ps, the structural shape changes (Figure 3a1, 3b1, 3c1, 3d1) corresponding to the number of FCC structural units changing from 1 FCC to 1, 0, 1, 3 FCC; HCP changing from 7 HCP to 2, 5, 3 HCP; BCC changing from 2 BCC to 2, 9, 1 BCC; Amor varies from 5110 Amor to 5116, 5114, 5113 Amor (Figures 3a2, 3b2, 3c2, 3d2) and the radial distribution function with Cu-Cu bond length varies from 2.54 Å to 2.54, 2.59, 2.59 Å and $g(r)$ varies from $g(r) = 4.22$ to 4.13, 4.18, 4.12 (Figures 3a3, 3b3, 3c3, 3d3). It should be clarified that the numbers '1 to 3 FCC' do not denote individual atoms, but rather represent the nucleation of distinct crystalline FCC clusters (nanocrystallites) emerging within the predominantly amorphous matrix. While the nanorod remains largely amorphous due to high surface energy and rapid thermal quenching constraints, the increase from 1 to 3 stable FCC clusters at 650 K indicates the critical onset of structural ordering (crystallization). This state is defined as 'optimal' because it yields the highest density of stable crystalline nuclei before thermal coiling or structural collapse occurs at higher temperatures. The results show that increasing the annealing time increased the Cu-Cu bond length from 2.54 Å to 2.59 Å, indicating that in the initial state the bond length had not yet reached a stable state corresponding to the number of structural units 5110 Amor. Increasing the annealing time gradually decreased the number of structural units from 5116 to 5113 Amor. These results highlight the importance of selecting an appropriate annealing time. Insufficient annealing leads to incomplete structural recovery, while excessive annealing does not significantly enhance stability and may increase computational cost.

3.4. Combined Effects of Temperature and Annealing Time

The interplay between temperature and annealing time determines the overall structural evolution of the copper nanorod. The results indicate that neither parameter alone is sufficient to achieve optimal structural stability. At the lower temperature of 600 K, increasing annealing time improves structural ordering, but the overall effect is limited due to insufficient atomic mobility. At high temperature (700 K), even long annealing times cannot fully restore order due to excessive thermal disorder. At intermediate temperature (650 K), the combination of adequate atomic mobility and controlled thermal energy enables efficient defect annihilation and structural reorganization. When combined with an annealing time of approximately 28 ps, this condition yields the most stable structure with the lowest energy and highest FCC fraction. This synergy reflects the competition between thermodynamic stabilization and kinetic disordering mechanisms. Temperature provides the energy needed for atomic motion, while annealing time allows sufficient duration for atoms to reach equilibrium configurations.

3.5. Energy Evolution and Structural Stability

The evolution of total energy provides a quantitative measure of system stability. In all cases, the total energy initially increases during heating due to enhanced atomic vibrations. During annealing, the energy gradually decreases as the system relaxes and defects are eliminated. At 650 K, the energy reduction is most significant, indicating efficient structural optimization. In contrast, at 700 K, the energy remains relatively high due to persistent disorder. The correlation between energy and structural metrics (RDF, CNA) confirms that lower energy states correspond to more ordered structures. This relationship highlights the importance of energy minimization in achieving stable configurations. Energy–Amorphization Correlation: A strong correlation is observed between the potential energy evolution and the amorphous fraction. As the amorphous content increases, the potential energy rises due to the loss of crystalline bonding efficiency. The minimum energy state obtained at 650 K and 28 ps corresponds to the maximum FCC fraction, confirming that structural ordering is energetically favorable. This relationship suggests that potential energy can serve as a predictive indicator of thermal stability in Cu nanorods.

3.6. Mechanism of Structural Evolution

The structural evolution observed in this study can be explained by the following mechanisms:

Thermal Activation: Increasing temperature enhances atomic vibrations and diffusion.

Defect Migration and Annihilation: Annealing allows defects such as vacancies and dislocations to migrate and annihilate [41].

Recrystallization: At optimal conditions, atoms rearrange into a more ordered FCC structure.

Amorphization at High Temperature: Excessive thermal energy disrupts atomic ordering, leading to partial amorphization. These mechanisms collectively determine the final structure of the system. The 'optimal condition' in this study is strictly defined based on two quantitative criteria: maximum structural ordering (highest FCC atomic fraction) and minimum potential energy. At 650 K and 28 ps, the nanorod system achieves its energy minimum (-3.42 eV/atom), indicating that internal stresses have been fully relaxed. Concurrently, the FCC crystal lattice reaches its peak fraction, and defect structures (amorphous surface states and unstable BCC configurations) are minimized. Below 650 K, the thermal energy is insufficient to overcome the activation barriers for defect annihilation, whereas at 700 K, excessive thermal vibrations disrupt the crystal lattice, leading to partial amorphization.

3.7. Proposed Structural Evolution Mechanism

Based on the RDF, CNA, and energy analyses, a three-stage structural evolution mechanism is proposed:

Stage I: Thermal Activation: Increasing temperature activates atomic vibrations and promotes defect migration.

Stage II: Defect Annihilation and Reordering: At intermediate temperatures (around 650 K), vacancies and stacking faults are eliminated, resulting in enhanced FCC ordering and reduced potential energy.

Stage III: Surface-Induced Amorphization: At temperatures approaching 700 K, excessive thermal fluctuations destabilize surface atoms. The disorder propagates toward the interior region, generating amorphous domains and reducing long-range crystallinity.

This mechanism highlights the competing effects between thermodynamic stabilization and thermal disordering during annealing.

4. Conclusion

The present work systematically investigates the temperature–time dependent structural stability of Cu nanorods. The results reveal that the competition between thermally activated atomic diffusion and surface-induced disorder governs the crystalline-to-amorphous transition. An optimal annealing condition of 650 K for approximately 28 ps was identified, corresponding to the minimum potential energy and maximum FCC ordering. These findings provide fundamental atomistic insights into thermal stability engineering of Cu nanostructures and may serve as a guideline for the design of Cu-based nanoelectronic and thermal-management devices.

Funding: The authors declare that no funds, grants, or other support were received during the preparation of this manuscript.

Data Availability Statement: The data that support the findings of this study are available from the corresponding authors upon reasonable request.

Declaration of competing interest: The authors declare that they have no known competing financial interest or personal relationships that could have appeared to influence the work reported in this paper.

References

- [1] G. Rodríguez-López, K. Martens, E.E. Ferrero, 2023. Temperature dependence of fast relaxation processes in amorphous materials. *Physical Review Materials*, 7, 105603. <https://doi.org/10.1103/PhysRevMaterials.7.105603>
- [2] K.K. Alaneme, E.A. Okotete, (2019). Recrystallization mechanisms and microstructure development in emerging metallic materials: A review. *Journal of Science: Advanced Materials and Devices*, 4(1), 19-33. <https://doi.org/10.1016/j.jsamd.2018.12.007>
- [3] Y. Tamai, (2017). Molecular dynamics simulations of structural transitions of crystalline polystyrene in response to external stresses and temperatures. *Polymer*, 128, 177–187. <https://doi.org/10.1016/j.polymer.2017.09.028>
- [4] Y.S. Li, Y. Zhang, N.R. Tao, K. Lu, (2008). Effect of thermal annealing on mechanical properties of a nanostructured copper prepared by means of dynamic plastic deformation. *Scripta Materialia*, 59(4), 475–478. <https://doi.org/10.1016/j.scriptamat.2008.04.043>
- [5] M. Thomas, H. Salvador, T. Clark, E. Lang, K. Hattar, S. Mathaudhu, (2023). Thermal and Radiation Stability in Nanocrystalline Cu. *Nanomaterials*, 13(7), 1211. <https://doi.org/10.3390/nano13071211>

- [6] M. Iqbal, E.d.F. Martins, N. Todorova, Z. Fu, I. Cole, P. Ordejón, (2026). Atomistic modeling of molecular interactions with copper oxides for corrosion inhibition. *npj Materials Degradation*.
<https://doi.org/10.1038/s41529-026-00779-8>
- [7] A. Soon, M. Todorova, B. Delley, C. Stampfl, (2007). Thermodynamic stability and structure of copper oxide surfaces: A first-principles investigation. *Physical Review B*, 75, 125420.
<https://doi.org/10.1103/PhysRevB.75.125420>
- [8] F. Granberg, S. Parviainen, F. Djurabekova, K. Nordlund, (2014). Investigation of the thermal stability of Cu nanowires using atomistic simulations. *Journal of Applied Physics*, 115, 213518.
<https://doi.org/10.1063/1.4876743>
- [9] Y. Xia, J. Zuo, C. Yang, K. Wu, G. Liu, J. Sun, (2023). Influence of thermal annealing on the microstructure evolution, fracture and fatigue behavior of nanocrystalline Cu films. *Materials Today Communications*, 36, 106793. <https://doi.org/10.1016/j.mtcomm.2023.106793>
- [10] L. Zhang, C.B. Zhang, Y. Qi, (2009). Molecular-dynamics investigation of structural transformations of a Cu₂₀₁ cluster in its melting process. *Physica B: Condensed Matter*, 404(2), 205–209.
<https://doi.org/10.1016/j.physb.2008.10.028>
- [11] D. Sharma, B.K. Pandey, R.L. Jaiswal, J. Gupta, S. Shukla, (2024). Studies on thermal conductivity of metallic nanoparticles with varying shape and size. *Chemical Physics Letters*, 846, 141363.
<https://doi.org/10.1016/j.cplett.2024.141363>
- [12] X. Zeng, F. Li, X. Zhou, W. Yan, J. Li, D. Yang, Q. Shen, X. Wang, M. Liu, (2023). The phase stability at intermediate-temperature and mechanical behavior of the dual-phase AlCoCr_{0.5}FexNi_{2.5} high entropy alloys. *Materials Chemistry and Physics*, 297, 127314.
<https://doi.org/10.1016/j.matchemphys.2023.127314>
- [13] Z. Mingxin, (2024). Heat Treatment of Metal. In: X. Kuangdi (Ed.), *The ECPH Encyclopedia of Mining and Metallurgy*. Springer, Singapore. https://doi.org/10.1007/978-981-99-2086-0_882
- [14] P. Jenei, C. Kádár, G. Han, P. Tran Hung, H. Choe, J. Gubicza, (2020). Annealing-induced changes in the microstructure and mechanical response of a Cu nanofoam processed by dealloying. *Metals*, 10(9), 1128.
<https://doi.org/10.3390/met10091128>
- [15] R.B. Godiksen, Z.T. Trautt, M. Upmanyu, J. Schiøtz, D. Juul Jensen, S. Schmidt, (2007). Simulations of boundary migration during recrystallization using molecular dynamics. *Acta Materialia*, 55(18), 6383–6391. <https://doi.org/10.1016/j.actamat.2007.07.055>
- [16] Z. Zhang, F. Ji, B. Jiang, H. Yu, L. Chen, K. Jiang, S. Lin, M. Jin, Z. Hu, (2025). Temperature-induced phase transition dynamics in large-sized GeTe single crystals: Multimodal insights from XRD and Raman spectroscopy. *Journal of Alloys and Compounds*, 1043, 184282.
<https://doi.org/10.1016/j.jallcom.2025.184282>
- [17] X. Tong, G. Wang, Z.H. Stachurski, J. Bednarčík, N. Mattern, Q.J. Zhai, J. Eckert, (2016). Structural evolution and strength change of a metallic glass at different temperatures. *Scientific Reports*, 6, 30876.
<https://doi.org/10.1038/srep30876>
- [18] X. Sun, S. Fan, M. Peng, L. Ma, L. Shen, H. Qi, Y. Zhao, M. Li, (2024). Classical molecular dynamics simulation of atomic structure transitions in FeSiCuMgAl high-entropy alloys under biaxial stretching. *Materials Today Communications*, 40, 109716. <https://doi.org/10.1016/j.mtcomm.2024.109716>
- [19] D. Fieser, K. Yin, H. Shortt, U. Dewanjee, B. Steingrímsson, I. N. Ivanov, J. Burns, P. K. Liaw, J.-M. Zuo, A. Hu, (2025). Surface Nanostructure Control and Thermodynamic Stability Analysis of Femtosecond Laser

- Ablated CuCoMn_{1.75}NiFe_{0.25} Nanoparticles. *Langmuir*, 41(50), 34173–34188. <https://doi.org/10.1021/acs.langmuir.5c05617>
- [20] T. Yoshiie, Y. Satoh, Q. Xu, (2004). Analysis of defect structural evolution in fcc metals irradiated with neutrons under well defined boundary conditions. *Journal of Nuclear Materials*, 329-333(Pt A), 81–87. <https://doi.org/10.1016/j.jnucmat.2004.04.006>
- [21] W. Liu, X. Zhang, H. Guo, X. Zhang, B. Yang, J. Ma, J. Chen, Y. Luo, F. Liu, (2026). Effect of flash-annealing on the microstructures and mechanical properties of Cu alloys. *Journal of Alloys and Compounds*, 1059, 186809. <https://doi.org/10.1016/j.jallcom.2026.186809>
- [22] M. S. Daw, M. I. Baskes, (1984). Embedded-atom method: Derivation and application, *Physical Review B*, 29(12), 6443–6453. <https://journals.aps.org/prb/abstract/10.1103/PhysRevB.29.6443>
- [23] Y. Mishin, M.J. Mehl, D.A. Papaconstantopoulos, A.F. Voter, J.D. Kress, (2001). Structural stability and lattice defects in copper: Ab initio, tight-binding, and embedded-atom calculations. *Physical Review B*, 63, 224106. <https://doi.org/10.1103/PhysRevB.63.224106>
- [24] S.M. Foiles, M.I. Baskes, M.S. Daw, (1986). Embedded-atom-method functions for the fcc metals Cu, Ag, Au, Ni, Pd, Pt, and their alloys. *Physical Review B*, 33, 7983–7991. <https://doi.org/10.1103/PhysRevB.33.7983>
- [25] H. Zhang, K. Chen, C. Kang, H. Liu, (2024). Atomic-scale understanding of microstructural evolution in electrochemical additive manufacturing of metallic nickel. *Materials & Design*, 245, 113288. <https://doi.org/10.1016/j.matdes.2024.113288>
- [26] R. Gupta, A.Gupta, A.K. Nigam, G. Chandra, 2001. Effect of induced disorder on low temperature resistivity of some non-magnetic and magnetic metallic glasses. *Journal of Alloys and Compounds*, 326(1–2), 275–279. [https://doi.org/10.1016/S0925-8388\(01\)01283-X](https://doi.org/10.1016/S0925-8388(01)01283-X)
- [27] J. Li, F. Chu, Y. Feng, 2023. Effect of atomic diffusion on interfacial heat transfer and tensile property of copper/aluminum composites. *Materials Today Communications*, 36, 106757. <https://doi.org/10.1016/j.mtcomm.2023.106757>
- [28] M. Boswell, M. Xu, S. M. Hus, A. M. dos Santos, W. Xie, (2026). Temperature-Dependent Structural Transition in Cu-Intercalated Trigonal CuYbSe₂. *Chemistry of Materials*, 38(1), 328–335. <https://doi.org/10.1021/acs.chemmater.5c02470>
- [29] F. Montheillet, (2023). Dynamic Recrystallization Behaviours in Metals and Alloys. *Materials*, 16(3), 976. <https://doi.org/10.3390/ma16030976>
- [30] N. V. Priezjev, (2018). Molecular dynamics simulations of the mechanical annealing process in metallic glasses: Effects of strain amplitude and temperature. *Journal of Non-Crystalline Solids*, 479, 42–48. <https://doi.org/10.1016/j.jnoncrysol.2017.10.009>
- [31] K. R. Kadhim, R. Y. Mohammed, (2022). Effect of Annealing Time on Structure, Morphology, and Optical Properties of Nanostructured CdO Thin Films Prepared by CBD Technique. *Crystals*, 12(9), 1315. <https://doi.org/10.3390/cryst12091315>
- [32] T. Konkova, S. Mironov, A. Korznikov, M. M. Myshlyaev, S. L. Semiatin, (2013). Annealing behavior of cryogenically-rolled copper. *Materials Science and Engineering: A*, 585, 178–189. <https://doi.org/10.1016/j.msea.2013.07.042>
- [33] A. D. Phan, D. T. Nga, N. T. Que, H. Peng, T. Norhourmour, L. M. Tu, (2025). A multiscale approach to structural relaxation and diffusion in metallic glasses. *Computational Materials Science*, 251, 113759. <https://doi.org/10.1016/j.commatsci.2025.113759>

- [34] U. Saraç, C.A. Tran, N.T. Giang, & Ş. Tălu, (2025). Influence of copper electrode material on surface quality in EDM drilling of heat-treated C45 steel. *Journal of Nanomaterials and Applications*, 1(1), 33–42. <https://doi.org/10.65273/hnit.jna.2025.1.33-42>
- [35] D.N. Trong, Q.T. Tran, & Ş. Tălu, (2025). Influence of Structural Configurations, Boundary Conditions, and Atomic Number on the Curie Transition Temperature of Bulk Cobalt: A Monte Carlo Simulation Study. *Nano*, 20(08), 2550012. <https://doi.org/10.1142/S1793292025500122>
- [36] T. Tran Quoc, D. Nguyen Trong, V. Cao Long, U. Saraç, Ş. Tălu, (2022). A Study on the Structural Features of Amorphous Nanoparticles of Ni by Molecular Dynamics Simulation. *Journal of Composites Science*, 6(9), 278. <https://doi.org/10.3390/jcs6090278>
- [37] V. C. Long and D. Nguyen Trong, (2023), Molecular Dynamics Approach to Processes in Bulk Au Materials, *Acta Phys. Pol. A*, 143(6), S191, Jun. <https://doi.org/10.12693/APhysPolA.143.S191>.
- [38] Y. Mishin, et al. (2001). Structural stability and lattice defects in copper: Ab initio, tight-binding and embedded-atom calculations. *Physical Review B*, 63(22), 224106, <https://journals.aps.org/prb/abstract/10.1103/PhysRevB.63.224106>
- [39] J. Zhang, X. Wang, Y. Zhu, T. Shi, Z. Tang, M. Li, G. Liao, (2018). Molecular dynamics simulation of the melting behavior of copper nanorod. *Computational Materials Science*, 143, 248–254. <https://doi.org/10.1016/j.commatsci.2017.11.011>
- [40] T. Xie, H. Zhang, J. Zhou, W. Sun, L. Ma, L. Cao, J. Yang, (2021). A stable Cu-polyatomic-cluster catalyst: Critical for methanol reforming deNO_x at mild temperature. *Applied Surface Science*, 563, 150321. <https://doi.org/10.1016/j.apsusc.2021.150321>
- [41] H. Shen, J. Yang, W. Li, (2025). Defect Annihilation Mechanisms in Hexagonal Cylinders Formed by Diblock Copolymers under Triangular Confinement. *Macromolecules*, 58(1), 439–450. <https://doi.org/10.1021/acs.macromol.4c02220>